Coastal Engineering 71 (2013) 1–12

Contents lists available at SciVerse ScienceDirect

Coastal Engineering

journal homepage: www.elsevier.com/locate/coastaleng

RANS v^2–f simulation of a swash event: Detailed flow structure

J. Desombre *, D. Morichon, M. Mory

Laboratoire SIAME, Université de Pau et des Pays de l'Adour, Anglet, France

ARTICLE INFO

Article history:
Received 28 July 2011
Received in revised form 24 May 2012
Accepted 8 July 2012
Available online 15 August 2012

Keywords:
Swash flow
Numerical simulation
RANS v^2–f turbulence model
Aeration
Flow reversal
Bed shear stress

ABSTRACT

The flow structure of a swash event over a uniform slope is studied using a RANS-VOF numerical model coupled with a v^2–f turbulence closure. The model is compared with experimental data of recent laboratory experiments. The ability of the turbulence modelling for simulating swash flow and the evolution of the computed bed shear stress during run-up and run-down are investigated. The agreement between numerical results and measured data, such as water depth, depth-averaged velocity and bed shear stress is very good during run-up. Main discrepancies are found during run-down. The paper also examines the aeration of the water layer in the swash flow, taking advantage of the PLIC method for computing the air–water interfaces. Air is continuously entrapped in the swash front and released at its rear during run-up. A detailed analysis indicates that the flow reversal is initiated near the bottom at the outer boundary of the swash zone and progresses landward. The study highlights the asymmetry between run-up and run-down. During run-up, the swash front propagation determines the turbulence properties and the bed shear stress profile on the beach, whereas the flow properties are more homogeneously distributed in the swash area during run-down.

1. Introduction

The swash zone is the part of the beach which is alternately covered and uncovered by water flow. In a recent review, Masselink and Puleo [16] have described the swash zone as the region of the near-shore where beach morphodynamic changes are the most dynamic. The swash zone is also considered as one of the most scientifically challenging oceanic environment for describing sediment transport [22]. Field measurements have shown important sediment flux in the swash zone with sediment concentrations generally up to one order of magnitude larger than those in the surf zone [9,7].

A precise description of the physical processes driving the swash motion is a prerequisite for modelling morphodynamic beach changes. A focus is put in this paper on turbulence effects and on the aeration of water during swash. In their review, Elfrink and Baldock [7] identified a series of potential sources of turbulence: the inner surf zone, the initial bore collapse at the shoreline, the boundary layer, the backwash bore and the swash–swash interactions. Swash–swash interactions are not in the scope of our study, since we only consider a single swash event. Since about 50 years, the idealised case of a swash flow generated by a bore collapse on a slope has been much studied. Because a bore is easily produced in the laboratory via a dam-break event into quiescent water, it was studied extensively theoretically, experimentally and numerically. The present paper continues previous work by Mory et al. [18] and we will not repeat here the literature review of the physics of bore collapse given in that paper. The numerical study of Mory et al. [18] focused on the transition process of bore collapse leading to the swash flow. Unlike predicted by the theory of Whitham [26], they showed that the bore collapse phenomenon is not completed at the position of shoreline at rest, but further upslope. The literature review on the bed boundary layer behaviour in the swash zone is sparse. Barnes [3] made direct bed shear stress measurements for various laboratory swash conditions. He found that "*run-up bed shear stress is typically greater than the peak backwash bed shear stress by at least a factor of two and up to a factor of four*". In most numerical studies, the velocity profile close to the bed is modelled using a wall function parametrization. The difficulty to achieve a reliable hydrodynamics description near the bottom mainly comes from the high variability of the flow, especially at high Froude number $Fr_o = U/\sqrt{gH_o}$. H_o is the water depth over which the bore propagates shorewards, U the bore propagation speed at the shoreline and g the acceleration of gravity. According to the literature review by Mory et al. [18], "*strong bores*", which are fully developed turbulent flows, are obtained for $Fr_o > 1.33$.

The numerical simulations presented by Mory et al. [18] were based on the laboratory test case of Yeh et al. [27] ($Fr_o = 1.43$). This test case was also taken by Zhang and Liu [28] to achieve numerical simulations using the COBRAS RANS-VOF code. The simulation of Mory et al. [18] examined the evolution of bed shear stress during run-up and run-down, but the study remained partly inconclusive due to the absence of bed shear stress data for the laboratory experiment of Yeh et al. [27]. A series of new laboratory data have been

* Corresponding author at: Laboratoire SIAME, ISA-BTP, Université de Pau et des Pays de l'Adour, Allée du Parc Montaury, 64600 Anglet, France. Tel.: +33 5 59 57 44 35.
E-mail addresses: jonathan.desombre@univ-pau.fr (J. Desombre), denis.morichon@univ-pau.fr (D. Morichon), mathieu.mory@univ-pau.fr (M. Mory).

0378-3839/$ – see front matter
http://dx.doi.org/10.1016/j.coastaleng.2012.07.001

recently documented which offer a new potential for testing numerical models and improving our knowledge of the physics of swash flows. O'Donoghue et al. [19] performed large scale swash laboratory experiments, which provide detailed flow structure data. With the same experimental setup, Barnes et al. [5] used a shear plate to measure the bed shear stress. Meanwhile, Sou et al. [23] and Sou and Yeh [24] studied the evolution of turbulence levels during swash motion using laboratory PIV measurements.

This paper presents results of simulations obtained using the THETIS code developed by the TREFLE laboratory (Bordeaux, France). The code performs a Volume Of Fluid (VOF) modelling of air–water flow with turbulence taken into account through a RANS approach coupled with the v^2-f model [6]. Previous studies by Lubin et al. [13–15] have shown that this code can be successfully used for simulating coastal hydrodynamics processes. Results of the numerical simulation are presented here and compared with the recent laboratory experiments of O'Donoghue et al. [19]. A primary focus is on air–water interfaces. Former computations of Mory et al. [18] were based on a Total Variation Diminishing (TVD) method, which presents the disadvantage of enhancing diffusion of the interface. The Piecewise Linear Interface Calculation (PLIC) method was successfully implemented to obtain the results presented here, allowing to examine in detail the evolution of aeration in the water layer during the swash event. Another focus of the paper is on bed shear stress results, which are computed during run-up and run-down flows. We compare our simulations results with the experimental data of Barnes et al. [5]. The results of the v^2-f turbulence model for this particular case are discussed. This model differs from the usual $k-\varepsilon$ model by solving the decay of turbulence in the viscous boundary layer, whereas the $k-\varepsilon$ model applies a wall law stating the properties of turbulence at the wall.

In the following section, we present the test case and the characteristics of the RANS-VOF model used in this study with a particular attention dedicated to the description of the v^2-f turbulence closure model. Swash flow structure computed by the model and comparisons with laboratory measurements are presented in Section 3. Finally, conclusion is given in Section 4.

2. Numerical modelling

2.1. Test case

The laboratory experiment of O'Donoghue et al. [19] was carried out in the long flume of the University of Aberdeen to study swash zone hydrodynamics. Bore collapse and subsequent run-up and run-down over an impermeable slope were generated by a dam-break mechanism as sketched in Fig. 1. While different bed roughnesses were experimented by O'Donoghue et al. [19], only the smooth slope case with perspex panels is considered in this paper. The setup consists of a water reservoir of length $L_T = 1$ m, placed at one end of a 20 m long flume. The reservoir is fronted by a gate designed to be raised rapidly. The initial water depth in the reservoir is $H_T = 0.65$ m while the water level in the other part of the flume is $H_o = 0.06$ m. The bottom of the flume is horizontal over a length $L_o = 3.8$ m, and then sloping at 1 : 10. When the gate is released, a large-scale solitary bore is generated and propagates towards the beach where it collapses, producing a swash event over the slope.

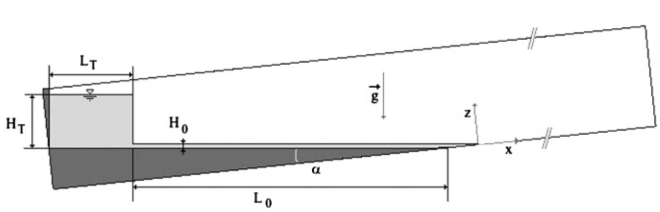

Fig. 1. Numerical setup adapted from the experimental setup of O'Donoghue et al. [19].

The experimental conditions used in O'Donoghue et al. [19] correspond to a high initial depth ratio $H_T/H_o = 10.8$ compared to the previous similar laboratory study of Yeh et al. [27] ($H_T/H_o < 2.8$). Applying the shallow water theory [25], the height of the developed bore propagating over the horizontal part of the flume is estimated to $h_m = 0.25$ m, and its propagation speed to $U = 2.5 \mathrm{m.s}^{-1}$. This corresponds to a Froude number $Fr_o = U/\sqrt{gH_o} = 3.28$ (see [18] for a summary of analytical theories establishing the values of U, h_m and Fr_o for the conditions of the experiment considered here). The laboratory conditions of O'Donoghue et al. [19] therefore generate a particularly strong bore, which can still be considered as representative of large swash events in the field [7]. The large flume horizontal length L_o enables the bore to be established before it reaches the shoreline. However, due to the finite volume of the reservoir, the lack of fluid behind the bore produces a swash lens that might be shallower than those occurring in the field.

Fig. 1 shows the domain of computation considered for simulations. The x axis is parallel to the sloping beach, positive shoreward, and with the origin set at the position of the shoreline at rest. The flume bottom and the solid left side of the reservoir are simulated as a porous medium with permeability asymptotically set to zero, thus imposing zero velocity for the fluid within them. The time $t = 0$ corresponds to the instant of gate opening.

The horizontal grid size is equal to $\Delta x = 5.10^{-3}$m for the entire computational domain. As explained in Section 2.3, the v^2-f turbulence model requires an extremely fine mesh near the bottom. For our test case, the vertical grid step grows exponentially with a ratio less than 1.3 between two successive grid cells (i.e. $\Delta z_{j+1} < 1.3\Delta z_j$), starting from $\Delta z = 10^{-5}$m at the bed up to $\Delta z = 10^{-2}$m at $z = 10$ cm. Above $z = 10$ cm, the vertical grid step is fixed to $\Delta z = 10^{-2}$m.

2.2. Governing equations

The velocity vector $\mathbf{U}(x,z,t)$ and pressure $p(x,z,t)$ variations are computed by solving the momentum equation

$$\rho\left(\frac{\partial \mathbf{U}}{\partial t} + (\mathbf{U}.\nabla)\mathbf{U}\right) = -\nabla\left(p + \frac{2}{3}\rho k\right) + \rho\mathbf{g} + \nabla.\left((\mu + \mu_t)\left(\nabla\mathbf{U} + \nabla^t\mathbf{U}\right)\right) \tag{1}$$

coupled with incompressibility

$$\nabla.\mathbf{U} = 0 \tag{2}$$

which are solved in this paper in two dimensions in a plane (O,x,z). ρ denotes the fluid density and μ the viscosity. Turbulence is accounted for using a Reynolds Average Navier Stokes (RANS) approach, with k the Turbulent Kinetic Energy (TKE) per unit mass [$\mathrm{m}^2.\mathrm{s}^{-2}$] and μ_t the eddy viscosity. The time and space variations of turbulence properties are determined using the v^2-f closure model developed by Durbin [6] which, besides the TKE k, introduces three others quantities: the dissipation rate of TKE per unit mass ε [$\mathrm{m}^2.\mathrm{s}^{-3}$], the TKE $\overline{v'^2}$ of the velocity component perpendicular to the direction of mean motion [$\mathrm{m}^2.\mathrm{s}^{-2}$] and a dimensionless function f serving for redistributing the TKE between the velocity component parallel to the mean flow and the velocity components perpendicular to it.

The eddy viscosity is defined as

$$\mu_t = \rho C_\mu \overline{v'^2} T \qquad \text{with} \qquad T = max\left[\frac{k}{\varepsilon}, 6\sqrt{\frac{\nu}{\varepsilon}}\right]. \tag{3}$$

The variations in time and space of k, ε, $\overline{v'^2}$ and f are computed by solving the following set of equations:

$$\rho\left(\frac{\partial k}{\partial t} + \nabla.(\mathbf{U}k) - k\nabla.\mathbf{U}\right) = P_r - \rho\varepsilon + \nabla.((\mu + \mu_t)\nabla k) \tag{4}$$